Journal of Thermal Analysis and Calorimetry, Vol. 93 (2008) 2, 527–533

THERMAL STABILITY OF DNA IN DNA–INDUCED DOTAP LIPOSOME AGGREGATES

S. Zuzzi[1,2], *G. Onori*[1,2] *and C. Cametti*[3,4*]

[1]Dipartimento di Fisica, Università di Perugia and CEMIN (Centro Eccellenza Materiali Innovativi Nanostrutturati) Via A. Pascoli, 06123, Perugia, Italy
[2]INFM-CRS SOFT, Unità di Perugia, Italy
[3]Dipartimento di Fisica, Università di Roma 'La Sapienza', Piazzale A. Moro 5, 00185- Roma, Italy
[4]INFM-CRS SOFT, Unità di Roma 1, Italy

The influence on the melting of calf thymus DNA induced by cationic liposomes, commonly used in gene therapy, was studied by means of ultraviolet spectrophotometry and differential scanning calorimetry. Both the two methods reveal that DNA in DNA-induced liposome complexes undergoes a denaturation process at a much higher temperature than free DNA does. The extent of protection strongly depends on the charge ratio $R(+/-)$ of liposome–DNA complexes. In the case of dioleoyl trimethyl ammonium propane (DOTAP) liposomes, the maximum of the stabilization occurs at $R(+/-)=0.7$, where the DNA is still native up to temperatures higher than 100°C. This protection against denaturation up to higher temperatures might be of importance for bio-technological applications, such as biomolecular separation, antigene sequencing and for drug design purpose.

Keywords: *DNA–liposome aggregates, DNA melting*

Introduction

The conformational behavior of DNA molecules, in the presence of oppositely charged objects (compaction agents), has been studied extensively in recent years, because of both its technological and biomedical relevance [1, 2]. Thanks to the development of methods for DNA extraction and purification and, later, of the potential use of these systems as vehicles for gene delivery and gene transfection, a number of studies on the compaction of DNA by cationic species in bulk solution have appeared in the last few years [3, 4].

The interaction of DNA with this oppositely charged objects gives rise to a very complex phenomenology, depending on their physical-chemical properties and on their chemical nature. The shape, size and stability of the resulting aggregates depend on a delicate balance between different driving forces, mainly of electrostatic origin.

Recently, Zinchenko and Chen [5] have summarized this phenomenology and have classified these agents into four different kinds, according to their dimensionality. In particular, they refer to zero-dimensional (multivalent cations), one-dimensional (polycations with charges distributed along the polymer chain), two-dimensional (cationic surfaces) and three-dimensional (nano- or mesoscopic three-dimensional structures) agents.

In aqueous solution, DNA adapts a coil conformation with an intrinsic rigidity (mechanical component) and a repulsion between negatively charged segments (electrostatic component). With addition of different oppositely charged objects, DNA is compacted into condensates of various densities and intricate topological rearrangements, including DNA condensation [1], DNA compaction [6, 7], liposome-induced aggregation [8] and DNA–induced liposome fusion [9, 10].

The basic features of DNA condensation by multications (zero-dimensional objects) are well known. DNA chain in extended coil conformation undergoes compaction into a compact condensate and the DNA negative charges become neutralized by controions [11, 12]. This compaction is a process that takes place at the level of a single DNA chain, as an all-or-none type transition [6]. Moreover, it is known that the presence of these mono- and polyvalent cations can significantly influence the thermodynamic parameters of the DNA melting process, by shifting the equilibrium toward a stabilization of the helix form [13–16]. Hence, the presence of counterions (at low to moderate concentrations) stabilizes DNA structure and increases the temperature of melting [17].

The compaction of DNA employing polyelectrolytes (one-dimensional objects) has been widely studied [18]. This process becomes almost stoichiometric in terms of ratio between DNA charges and charges of the polycation and, in most cases, the to-

* Author for correspondence: cesare.cametti@roma1.infn.it

1388–6150/$20.00

Akadémiai Kiadó, Budapest, Hungary
Springer, Dordrecht, The Netherlands

roidal shape of the DNA condensate is not preserved. The all-or-none scenario changes into continuous DNA chain compaction [7, 19]. In this case, on the base of differential scanning calorimetry measurements, complexation of DNA with the cationic polymers, such as polyethylenimine (PEI) or poly-*L*-lysine (PLL), resulted in a decreased stability, when the DNA was in excess, although polymers stabilized DNA in the polymer excess condition [20]. Numerous studies have been undertaken on the behavior of DNA chains in the presence of cationic surfactants. In this case, the interaction takes place at level of monomer and a more compact and stable structure is observed, whose thermal denaturation occurs at temperatures higher than 100°C [21–24].

The less dense compaction of DNA chain on artificial nanoscale templates such as synthetic nanoparticles and nanotubes (three-dimensional objects) is nowadays much less studied and understood. There exist several important in vivo examples, where a DNA chain is compacted because of the interaction with nanoscale objects, forming complexes with a well defined molecular architecture [25, 26]. One of the well known manifestations of such a self-organization induced by nanoscale objects is the hierarchical DNA molecule assembly into a chromosome [27, 28].

Recent studies [8–10, 29–31] have analyzed the structures formed by interactions of DNA chains with several types of liposomes. In these cases, there are two differently organized complexes driven by the experimental conditions investigated: liposome excess or DNA excess conditions. In cationic liposome excess, DNA addition favors the formation of liposome clusters. In other words, liposomes, which maintain their integrity, aggregate, originating a cluster phase [8, 29, 31]. In DNA excess, the chains coexist in two different conformations: coil and globules. Moreover, during interactions between DNA and cationic liposomes, DNA compaction is accompanied by the liposome rupture, with the formation of DNA–lipid complexes of more complex structural organization [9, 10].

In the framework of this complex and intriguing background, in this work, the thermal melting of calf thymus DNA was investigated in the presence of varying concentrations of dioleoyl trimethyl ammonium propane (DOTAP) liposomes by means ultraviolet spectrophotometry (UV) and differential scanning calorimetry (DSC). The DNA–DOTAP liposome interaction was analyzed below and close the isoelectric condition (at which the negative charges of DNA and the positive charges of DOTAP liposomes are stoichiometrically equal). In this situation, i.e., DNA excess condition, structures with an overall negative charge (resembling the charge of the DNA chain), were observed [32]. Moreover, lipids favor the DNA compaction, inducting the collapse of DNA molecules from an extended coil conformation to a compacted globular state [32]. The aim of this study was to obtain information on the stability of DNA in the ctDNA/DOTAP liposome complexes and to investigate how this thermal stabilization depended on the charge ratio, in the vicinity of the isoelectric point.

Experimental

Materials and sample preparation

DOTAP was purchased from Avanti Polar Lipids (Alabaster, Al) and was used without further purification. Unilamellar liposomes were prepared by standard lipid film hydration method. The lipid was dissolved in chloroform methanol (1:1 vol/vol) and after 3 h vacuum evaporation of the organic solvents, the resulting lipid film was re-hydrated with Milli-Q quality water, (electrical conductivity less than $\sigma=10^{-6}$ Ω^{-1} cm^{-1}, at room temperature), to the final concentration of 1 mg mL^{-1}.

After solvent evaporation, dried lipid films were hydrated with deionized water, the re-hydration process was carried out for 1 h. In order to form unilamellar vesicles, the lipid solution was sonicated at a temperature of 25°C for 1 h at a pulsed-power mode until the solution appeared optically transparent in white light. The solution was filtered through Millipore polycarbonate filter 0.45 μm in size. Liposome size and size distribution obtained from dynamic light scattering measurements give an average diameter of about 50 nm, with a moderate polydispersity of about 0.2 (Fig. 1), as expected for a rather homogeneous particle suspension.

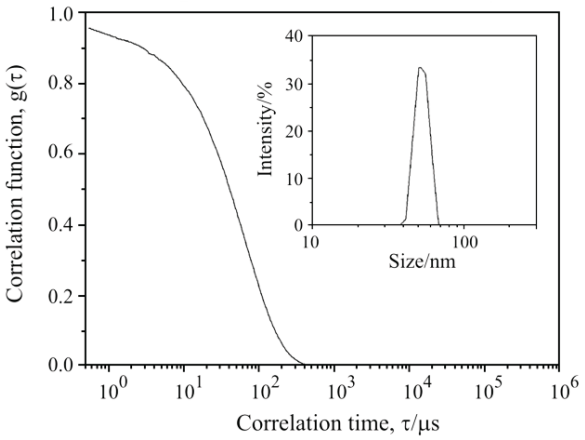

Fig. 1 Correlograms of the dynamic light scattering (DLS) measurements of DOTAP liposomes. The inset shows the liposome distribution size. The liposomes have an average diameter of about 50 nm with a moderate polydispersity of about 0.2

Double-stranded calf thymus DNA sodium salt, purchased from Sigma Chem. Co. and used without further manipulations, was dissolved in water. The purity of the DNA employed was analyzed by means ultraviolet spectrophotometry (A_{260}/A_{280}=1.9, with A_{260} and A_{280} absorbance at 260 and 280 nm, respectively).

DNA–DOTAP liposome interaction was obtained by adding varying amounts of DOTAP liposome suspension to a DNA solution at the fixed concentration. The complexes were prepared in the concentration range below the isoelectric condition, i.e. in DNA excess condition. The DNA concentration used, both for ultraviolet spectrophotometry and for differential scanning calorimetry measurements, was relatively low in order to avoid formation of a heavy precipitate.

Methods

Ultraviolet spectrophotometry (UV)

The absorption spectra have been recorded with a spectrophotometer Jasco-V-570 in an interval of wavelength from 200 to 350 nm. The molar concentration of DNA was determined from UV absorption at 260 nm, by using ε_{DNA}=6600 M^{-1} cm^{-1} [33]. Each sample was heated from 25 to 100°C, at intervals of 5°C, after 10 min of thermalization. In all the experiments, the DNA concentration was maintained constant to the value $4.95 \cdot 10^{-2}$ mg mL^{-1}, while the DOTAP concentration was varied from 0.031 to 0.28 mg mL^{-1}.

The DNA–lipid complexes, close to the isoelectric condition, when the negative charge along the DNA chains equals the positive charges on the liposome surfaces, presented a very large absorbance at larger wavelengths. This is caused by the large size of complexes (Mie regime) [34, 35] which in these conditions occurs. Therefore, the effective absorbance for DOTAP liposome–DNA complexes has been determined by subtracting to the measured absorbance a contribution with a wavelength dependence according to A/λ^{α} [36, 37], whose parameters, A and α were obtained by fitting the experimental values in the range of higher wavelengths (in the range from 320 to 350 nm).

Differential scanning calorimetry (DSC)

DSC experiments were performed on a Micro-DSC II Setaram calorimeter (Lyon, France). This instrument, calibrated with indium standard, has a resolution, in both heating and cooling cycles, better than 2 μW. The curves were recorded in the range from 20 to 100°C, at a heating rate, (dT/dt), of 0.5°C min^{-1}. DSC technique [38] measures the heat flow, dQ/dt, from which the excess heat capacity is obtained ($C_p^{ex}=dQ/dt(dT/dt)^{-1}n^{-1}$, with n=number of moles). A mass of 0.830 g of the sample and of the reference (water) was inserted in the sample and in the reference cells, respectively. The masses of the sample and of the reference cells were always matched. Each sample underwent two heating and cooling cycles. When the sample of DNA underwent the second thermal cycle until about 100°C, no heat absorption was revealed because of the denaturation of ctDNA is effectively irreversible on the time scale of these experiments. Taking into account that process of denaturation of DNA is an irreversible process, the excess power *vs*. temperature scan for the DNA and DOTAP–DNA complexes was obtained by subtracting the power input of the scan of second thermal cycle from the power input scan of the first cycle solution *vs*. solvent. For each sample, the peak height was measured. The transition temperature refers to the maximum of the excess heat capacity peak. The results were largely independent of DSC scan rate.

The lower limit of DNA concentration needed for a calorimetric measurement with our experimental set-up was of the order of 2.5 mg mL^{-1}. At such concentrations, interactions between DNA and DOTAP liposomes could occur not homogenously in the whole sample, because of the semi-dilute condition of DNA at these relatively high concentrations. Accordingly, we prepared samples at lower concentrations, by adding a DOTAP liposome suspension, at concentrations varying from 0.12 to 0.58 mg mL^{-1}, to DNA solution at a concentration of 0.38 mg mL^{-1}. The DOTAP liposome–DNA suspension has been, at a later time, concentrated under vacuum to the desired concentration value.

Results and discussion

Ultraviolet spectrophotometry

As is well known, DNA absorbance is attributed to nucleic bases which display an UV intense band of absorption at 260 nm. When calf thymus DNA is heated up to 100°C, an increase in absorption at 260 nm is observed, as is known from literature data [39].

The change in the absorbance at 260 nm of DOTAP liposome–DNA complexes as a function of temperature, from 20 to 100°C, at different charge molar ratios $R(+/-)$=[DOTAP]/[PO_4^-] are shown in Fig. 2. Here, [DOTAP] and [PO_4^-] are the DOTAP and DNA phosphate group molar concentrations in DOTAP liposome–DNA suspension respectively. In contrast with the significant hyper-chromicity effect of free DNA, the observed changes in UV absorption were much smaller when DNA chains interact with DOTAP liposomes, i.e., the presence of liposomes greatly reduced the extent of DNA denaturation

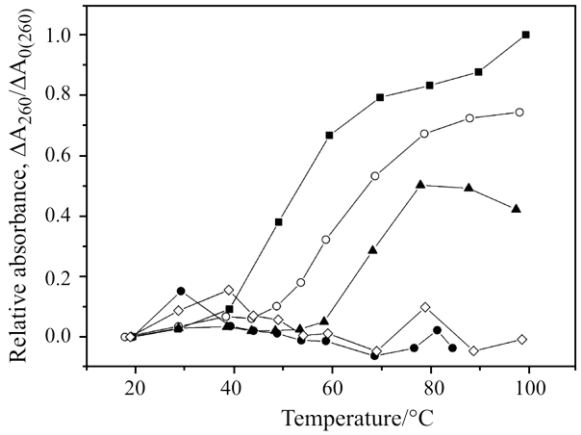

Fig. 2 The change in the absorbance, $\Delta A=A(T)-A(T=20)$, normalized to the absorbance of pure DNA, $\Delta A_0=A_0(T)-A_0(T=20)$, at a wavelength of 260 nm of DNA and DOTAP liposome–DNA complexes as a function of temperature. Each sample was heated from 25 to 100°C at intervals of 5°C, after 10 min of thermalization. The samples were prepared at several $R(+/-)$ molar ratios: ■ – $R(+/-)$= 0, pure DNA; ○ – $R(+/-)$= 0.3; ▲ – $R(+/-)$= 0.47; ◇ – $R(+/-)$= 0.7 and ● – $R(+/-)$= 2.64. The uncertainties are within 5–10%

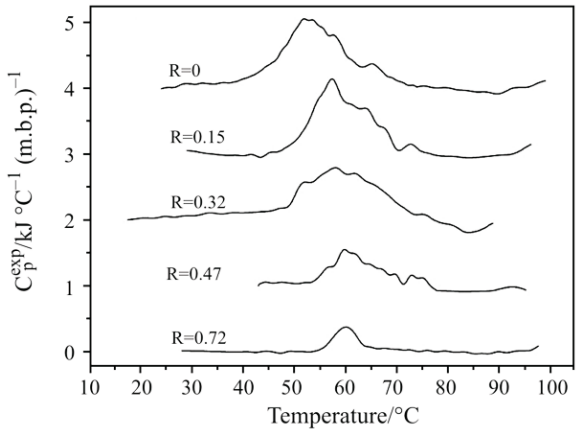

Fig. 3 Calorimetric heating scans of DNA and DOTAP liposome–DNA aggregates in aqueous solution, at a DNA concentration of 2.5 mg mL^{-1}. The curves are acquired at different DOTAP molar concentrations, varying the molar charge ratio $R(+/-)$ from 0 to 0.7. Curves have been shifted along the *y*-axis to avoid overlap and to facilitate visibility. Reproducibility was checked by repeated measurements

at 100°C. Moreover, the extent of protection depended strongly on the charge ratio $R(+/-)$ of DOTAP–DNA complexes. Figure 2 shows that the hyper-chromicity effect due to the thermal denaturation decreases with the increase of $R(+/-)$. When $R(+/-)$=0.7, the DNA is still all native up to temperatures as high as 100°C. This process is accompanied by a progressive shift of the melting temperature towards higher values.

DSC assay of DNA–lipid complexes

In order to study the effect of DOTAP liposomes on the stability of DNA and to further characterize the protection of DNA induced by the DOTAP liposomes, the thermal melting of ctDNA was investigated by DSC measurements, in the temperature range from 25 to 100°C, at different charge ratios $R(+/-)$. The curves of DNA and DNA DOTAP liposome complexes are shown in Fig. 3. All thermal curves have been shifted vertically for visual clarity.

Calf thymus DNA, exhibits a typical absorption curve with an asymmetrical melting band with several sub-transitions [40]. The individual peaks that occurred at different temperatures are due to the difference in the base composition and cover different areas because of the relative frequency of the particular repetitive sequences in terms of different GC content (in general in calf thymus DNA there is about 40% of GC bases pairs [41]). The calorimetric enthalpy, ΔH, (the area under the transition thermal profile) [42] is equal to 17.2 kJ mol^{-1}.

Figure 3 shows how the melting curve of ctDNA changes with the increase of the ratio $R(+/-)$ and therefore of the DOTAP liposome concentration in the liposome–DNA complexes. As can be seen, there is a progressive reduction of the decrease of the calorimetric enthalpy accompanied by an increase of the melting temperature, T_m, from 51.9 to 60.1°C.

These behaviors are in good qualitative agreement with the analysis of UV measurements where, with the decrease of the absorbance, it is concomitant the simultaneous decrease of the enthalpy. Figure 4 shows how both the normalized change of enthalpy, $\Delta H/\Delta H_0$, and the normalized change of absorbance,

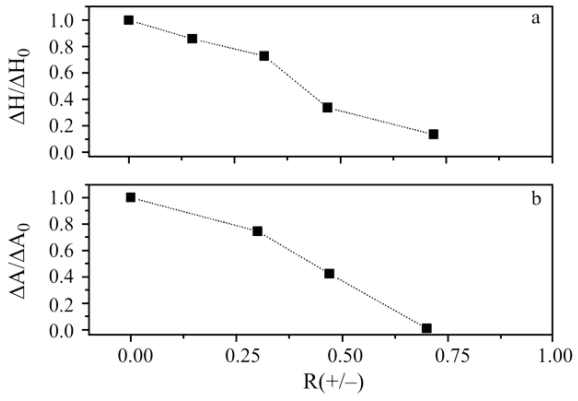

Fig. 4 a – Enthalpy ΔH normalized to the enthalpy ΔH_0 of pure DNA in the DNA-induced DOTAP liposome complexes as a function of the ratio $R(+/-)$. b – absorbance ΔA at 260 nm of DNA-induced DOTAP liposome complexes at the temperature of 100°C normalized to the absorbance ΔA_0 of pure DNA

$\Delta A/\Delta A_0$, at the temperature of 100°C, vary as a function of the ratio $R(+/-)$.

From our point of view, in agreement with a large experimental evidence on DNA interaction with lipids, the overall observed phenomenology suggests the formation of a complex that is thermally more stable, with a thermal denaturation above 100°C, out of the temperature range allowed by our experimental setup. Whereas the first transition is probably associated with melting around the un-complexed base pairs of DNA helices, the thermal stability, at higher temperatures, that we are not able to reach because of instrumental limitations, might be justified by a more effective packing of DNA between DNA–induced liposome complexes.

The same qualitative phenomenology has been observed by Tarahovsky *et al*. [43] for the DNA–EDOPC complexes, who observed the formation of new complexes with melting temperature at about 115°C and, more recently, by Akamatsu *et al*. [44], who report unusual enhanced thermal stability of a DNA duplex formed on a gold nanoparticle surface. A biphasic behavior of DNA complexed with cationic lipid DODAB was also observed by Mel'nikova *et al*. [45], who observed a main transition very close to the melting temperature of free DNA and a second transition at a higher temperature (in this case, this transition starts at about 76°C).

Recently, we have reported [32] a unified scenario of the DOTAP liposome–DNA complexation over an extended range of $R(+/-)$ ratios, obtained under different experimental conditions (DNA excess or DOTAP liposome excess conditions). The main results are summarized in Fig. 5, where we show the average size (and the ζ-potential) of the aggregates in the different regions relevant to this process. This region can be roughly divided into two regions, the former, at low $R(+/-)$, up to $R(+/-) \sim 0.15$, where there is the coexistence of free DNA and compacted DNA (DNA globules), and the latter, for $R(+/-)$ larger than 0.15, where the fraction of free DNA is lacking and all the DNA present is involved in the formation of DNA–induced liposome aggregates. In this region, the system undergoes the two typical phenomena of reentrant condensation (behavior of the hydrodynamic radius of the aggregates) and charge inversion (behavior of the ξ-potential of the aggregates) of charged colloidal systems. A sketch of the hypothesized structural arrangements occurring in DOTAP liposome–DNA aggregation is shown in Fig. 6.

It is worth noting that the thermal behavior of DNA is different both if DOTAP liposome interaction occurs at a single DNA chain level (DNA compaction) and if it occurs involving all the DNA present (DNA–induced liposome aggregates). From a calori-

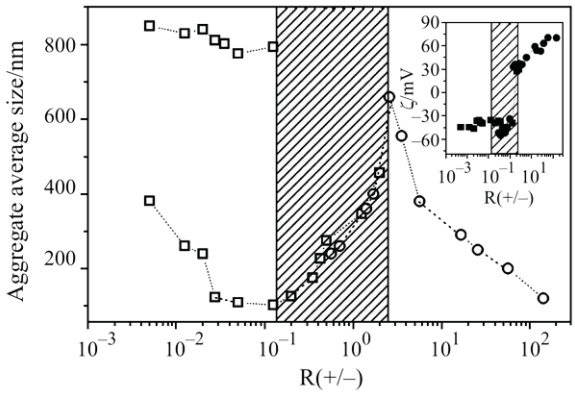

Fig. 5 The overall behavior of the complexation of DOTAP liposomes with DNA as a function of the molar charge ratio $R(+/-)$ (data from [32]). The dashed regions marks the range of $R(+/-)$ where UV and DSC measurements have been carried out. The data show the DNA compaction and the reentrant condensation in the DNA–induced liposome aggregates. The inset shows the charge inversion effect, revealed by the reversal sign of the ξ-potential

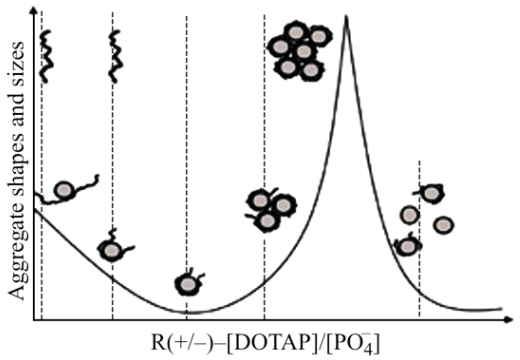

Fig. 6 A sketch of the possible structural arrangements during the DOTAP–DNA interactions as a function of the molar charge ratio $R(+/-)$. The typical size distribution observed in both the two regimes (DNA excess and DOTAP excess conditions) is also shown (continuous line)

metric point of view, the present results show that, with the beginning of the DNA–induced liposome aggregation ($R(+/-) \sim 0.15$), the thermal stability increases and denaturation less and less occurs (at the temperature of free DNA) until when, at the isoelectric point, no denaturation at all occurs, at least up to 100°C. In other words, the formation of the aggregates is concomitant with the thermal stability of the DNA chains, whose denaturation does not occur up to the temperature of 100°C. This is probably a result of the topological constraint imposed when the DNA is included within the liposome cluster aggregates, which reduces the cooperativity of base pair melting (and the gain in entropy).

Conclusions

Combined differential scanning calorimetric and ultraviolet spectroscopy measurements have evidenced that DNA, participating to complexes resulting from interactions with DOTAP liposomes, presents a very high thermal stability. The extent of thermal protection strongly depends on the molar charge ratio $R(+/-)$. For values of $R(+/-)$ larger than about 0.7, DNA is still native up to 100°C.

Previous measurements based on dynamic light scattering and radiowave dielectric spectroscopy [32] have evidenced, when cationic vesicles such as DOTAP liposomes are added to a DNA solution, the coexistence of some compacted DNA ('DNA globules') with DNA coils, yielding a population of DNA–liposome complexes in equilibrium with free DNA molecules. As can be seen in Fig. 5, for values of $R(+/-)$ above about 0.15, the free DNA component disappears and we observe the beginning of an aggregate formation. By means of differential calorimetry and ultraviolet spectroscopy, we have explored the region of $R(+/-)$ between 0.15 and 2.7. Our results show that, in the first part of this interval, for $R(+/-)$ lower than about 0.7, there is still a fraction that behaves, as far as the thermal denaturation is concerned, as a free DNA. The progressive decrease of the change in both the enthalpy and the absorbance indicates a progressive reduction of the fraction of free DNA. Above $R(+/-)=0.7$, when larger and more compact aggregates are formed, our measurements suggest that DOTAP liposomes–DNA complexes are protected against denaturation, up to, at least, 100°C. These results provide evidence that a complete thermal stabilization of DNA occurs only when rather large aggregates are formed.

A similar phenomenology has been observed in the interaction of DNA in the presence of surfactants, (two dimension compaction agents, according to the scheme given by Zinchenko [5]) where the thermal stabilization is already achieved at the formation of a compacted DNA structure. Whereas in this latter case, the resulting structural arrangements have been well described [46], interactions between DNA and cationic liposomes (three-dimensions compaction agents), in the condition of DNA excess, are not well understood yet. The establishment of more definitive relationships between the lipidic structure of liposomes and the thermal stability will require a further analysis of liposomes built up by a variety of head-groups and hydrophobic parts.

References

1 V. A. Bloomfield, Curr. Opin. Struct. Biol., 6 (1996) 334.
2 B. Lindman and K. Thalberg, Interactions of Surfactants with Polymers and Proteins, CRC, Boca Raton, FL 1993.
3 H. Peterson, K. Kunath, A. L. Martin, S. Stolnick, C. J. Roberts, M. C. Davies and T. Kissel, Biomacromolecules, 3 (2002) 926.
4 K. Eskilsson, C. Leal, B. Lindman, M. Miguel and T. Nylander, Langmuir, 17 (2001) 1666.
5 A. Zinchenko and N. Chen, J. Phys.: Condens. Matter, 18 (2006) R453.
6 K. Yoshikawa and Y. Yoshikawa, Pharmaceutical Perspectives of Nucleic Acid-Based Therapeutics, Taylor and Francis, London 2002.
7 A. A. Zinchenko, D. Baigl and Y. Yoshikawa, Polymeric Nanostructures and their Applications, American Scientific, Stenvenson Ranch, (CA) USA 2006.
8 S. Sennato, F. Bordi, C. Cametti, M. Diociaiuti and P. Malaspina, Biochim. Biophys. Acta, 1714 (2005) 11.
9 Y. Xu, S. W. Hui, P. Frederik and F. C. Szoka, Biophys. J., 77 (1999) 341.
10 M. T. Kennedy, E. V. Pozharski, V. A. Rakhmanova and R. C. MacDonald., Biophys. J., 78 (2000) 1620.
11 V. A. Bloomfield, Biopolymers, 44 (1998) 269.
12 D. Baigl and K. Yoshikawa, Biophys. J., 88 (2005) 3486.
13 G. L. Eichhorn and N. Davidson, J. Am. Chem. Soc., 90 (1968) 7323.
14 D. W. Gruenwedel, Biochim. Biophys. Acta, 340 (1974) 16.
15 J. Duguid, V. A. Bloomfield, J. Benevides and G. J. Thomas, Biophys. J., 65 (1993) 1916.
16 J. Duguid, V. A. Bloomfield, J. Benevides and G. J. Thomas, Biophys. J., 69 (1995) 2623.
17 V. A. Bloomfield, D. M. Crothers and J. I. Tinoco, Nucleic Acids: Structures, Properties, and Functions, University Science Books, Sausalito, (CA) USA 2000.
18 A. V. Kabanov and V. A. Kabanov, Bioconjugate Chem., 6 (1995) 7.
19 E.Wagner, M. Cotton, R. Foisner and M. L. Birnstiel, Proc. Natl Acad. Sci. USA, 88 (1991) 4255.
20 B. A. Lobo, S. A. Rogers, S. Choosakoonkriang, J. G. Smith, G. Koe and C. R. Middaugh, J. Pharm. Sci., 91 (2002) 454.
21 S. M. Melnikov, V. G. Sergeyev and K. Yoshikawa, J. Am. Chem. Soc., 117 (1995) 2401.
22 V. Kahl, J. O. Radler, K. Wagner, D. Harries, S. M. May and A. Ben-Shaul, Langmuir, 16 (2000) 303.
23 S. M. Melnikov, V. G. Sergeyev, K. Yoshikawa, H. Takahashi and I. Hatta, J. Chem. Phys., 107 (1997) 6917.
24 S. Marchetti, G. Onori and C. Cametti, J. Phys. Chem. B, 110 (2006) 24761.
25 M. E. Ceritelli, N. Cheng, A. H. Rosenberg, C. E. McPherson, F. P. Booy and A. C. Steven, Cell, 91 (1997) 217.
26 H. Schiessel, J. Phys.: Condens. Matter, 15 (2003) R699.
27 R. D. Kornberg, Science, 184 (1974) 868.
28 K. Luger, A. W. Mader, R. K. Richmond, F. D. Sargent and T. J. Richmond, Nature, 389 (1997) 251.
29 F. Bordi, C. Cametti, C. Marianecci and S. Sennato, J. Phys.: Condens. Matter, 17 (2005) S3223.
30 F. Bordi, C. Cametti and S. Sennato, Chem. Phys. Lett., 409 (2005) 134.

31 F. Bordi, C. Cametti, S. Sennato and D. Viscomi, J. Chem. Phys., 126 (2007) 024209.
32 S. Zuzzi, C. Cametti, G. Onori and S. Sennato, Phys. Rev. E, 76 (2007) 011925.
33 M. F. Rechmann, S. A. Rice, C. A. Thomas and P. Doty, J. Am. Chem. Soc., 76 (1954) 3047.
34 K. K. Mei, IEE Trans. Anten. Propagat., 22 (1974) 760.
35 G. Mie, Ann. Phys., 330 (1908) 377.
36 P. W. Barber and S. S. Hill, Light scattering by particles: Computational methods. World Scientific, Singapore 1990.
37 C. F. Bohren and D. R. Huffmann, Absorption and Scattering of Light by Small Particles, Wiley-Interscience, New York 1983.
38 L. Benoist, Thermochim. Acta, 163 (1990) 111.
39 A. Arco, M. Belli, F. Mazzei and G. Onori, Studia Biophysica, 78 (1980) 57.
40 R. G. Campisi, S. Fason and D. Grasso, Nuovo Cimento, 14 (1992) 851.
41 W. A. Rees, T. D. Yager, J. Korte and P. H. von Hippel, Biochemistry, 32 (1993) 137.
42 E. Freire and R. L. Biltonen, Crit. Rev. Biochem., 5 (1978) 85.
43 Y. S. Tarahovsky, V. A. Rakhmanova, R. M. Epand and R. C. MacDonald, Biophys. J., 82 (2002) 264.
44 K. Akamatsu, M. Kimura, Y. Shibata, S. Nakano, D. Miyoshi, H. Nawafune and N. Sugimoto, Nano Lett., 6 (2006) 491.
45 Y. S. Mel'nikova, S. M. Mel'nikov and J.-E. Lofroth, Biophys. Chem., 81 (1999) 125.
46 D. Liang, C. Burger, F. Yeh, S. Zhou and B. Chu, Biomacromolecules, 5 (2004) 1256.

Received: January 2, 2008
Accepted: February 28, 2008

DOI: 10.1007/s10973-008-9028-9